Am J Cancer Res 2019;9(11):2397-2412
www.ajcr.us /ISSN:2156-6976/ajcr0096739

Original Article

Benzethonium chloride suppresses lung cancer tumorigenesis through inducing p38-mediated cyclin D1 degradation

Xiao-Hui Huang[1], Yang Wang[1], Pan Hong[1], Jie Yang[1], Can-Can Zheng[1], Xing-Feng Yin[1], Wen-Bo Song[1], Wen Wen Xu[2], Bin Li[1], Qing-Yu He[1]

[1]*Key Laboratory of Functional Protein Research of Guangdong Higher Education Institutes, Institute of Life and Health Engineering, College of Life Science and Technology, Jinan University, Guangzhou 510632, China;* [2]*Institute of Biomedicine, Guangdong Provincial Key Laboratory of Bioengineering Medicine, National Engineering Research Center of Genetic Medicine, Jinan University, Guangzhou 510632, China*

Received May 9, 2019; Accepted June 13, 2019; Epub November 1, 2019; Published November 15, 2019

Abstract: Lung cancer is the leading cause of cancer-related deaths worldwide, but effective therapeutics is limited. This study aims to identify novel anticancer strategy from a Food and Drug Administration (FDA)-approved drug library consisting of 528 compounds. Benzethonium Chloride (BZN), a FDA-approved drug for anti-infective, was found to markedly induce apoptosis and inhibit proliferation and colony formation ability of lung cancer cells in dose- and time-dependent manners. BZN also enhanced the sensitivity of lung cancer cells to gefitinib, the first-line treatment strategy for selected lung cancer patients. Furthermore, BZN significantly delayed the growth of tumor xenografts in nude mice by increasing apoptosis and decreasing Ki-67 proliferation index, without obvious toxic effects to the vital organs of animals. Mechanistically, quantitative proteomics coupled with bioinformatics analyses and a series of functional assays demonstrated that BZN induced cell cycle arrest at G1 phase, and this was associated with an increase in p38-mediated phosphorylation at threonine 286 (T286) and accelerated degradation of cyclin D1. Our findings provide the first evidence that BZN could be a promising therapeutic agent in lung cancer treatment.

Keywords: Lung cancer, benzethonium chloride, cell cycle arrest, cyclin D1 degradation, gefitinib sensitivity, drug repurposing

Introduction

The incidence of lung cancer has dramatically increased over the last few decades and more than 2 million new cases are estimated to be diagnosed in 2018 worldwide [1, 2]. Non-small cell lung cancer (NSCLC) accounts for 85% of all cases of lung cancer and about 10% to 15% are small cell lung cancer (SCLC) [3]. Patients with lung cancer often present with advanced disease at initial diagnosis [4, 5]. At present, surgery remains the primary treatment option for lung cancer, and chemotherapy and radiotherapy are also used as adjuvant therapy to improve the treatment outcome. However, resistance of tumors to chemotherapy often occurs and many patients still relapse with more aggressive tumor phenotypes. Limited therapeutic options, chemoresistance and rapid metastasis lead to poor prognosis in lung cancer patients [6]. Therefore, development of novel treatment strategies is urgently needed for this lethal disease.

To find new uses for existing drugs outside the scope of the original indication, also known as drug repositioning, is an efficient method for obtaining more therapeutic drugs. A recent study reported that disulfiram, an old alcohol-aversion drug, can bind and immobilize NPL4 and trigger a heat-shock response, induce a complex cellular phenotype leading to cell death [7]. In present study, a drug library consisting of FDA-approved 528 small inhibitors was used to screen the compounds with anticancer property. We found that Benzethonium chloride (BZN), a quaternary ammonium salt, exerted a significant suppressive effect on tumorigenesis of lung cancer cells. BZN, a well-known surface antifungal and antibacterial

compound, has been approved by FDA for use in various anti-infective products and inhibits the response of acetylcholine in neuronal nicotinic acetylcholine receptors in a competitive and non-competitive manner [8]. However, the effect of BZN in cancer remains unclear and in particular, its anticancer function has not been reported in lung cancer. Here, *in vitro* and *in vivo* experiments were carried out to study whether BZN could be a new treatment option for lung cancer.

Quantitative proteomics provides a powerful tool to uncover the action mechanisms of anticancer compounds including BZN [9-11], which remains to be elucidated. Here, Stable Isotope Labeling by Amino Acids in Cell Culture (SILAC)-mass spectrometry (MS) coupled bioinformatics suggested that BZN may inhibit lung cancer cell proliferation through causing dysregulated cell cycle control. Cell cycle dysregulation is a common characteristic of human cancers that leads to uncontrolled cell proliferation and tumorigenesis. Cyclin D1 is a critical regulator of G1 to S phase transition, and plays an important role in development and progression of cancer [12]. Overexpression of cyclin D1 is frequently observed in various cancers [13], and deregulated protein degradation of cyclin D1 is one of the main reasons being responsible for the increased levels of cyclin D1 in cancer cells [14, 15]. Therefore, enhancement of cyclin D1 degradation may offer a useful strategy for therapeutic intervention [16]. The mechanism involved in the regulation of cyclin D1 stability has been well studied that phosphorylation of two key sites, threonine residue 286 (T286) and threonine residue 288 (T288), participate in cyclin D1 degradation. Cyclin D1 can be phosphorylated at T286 for its protein degradation by p38 and extracellular regulated protein kinase 2 (ERK2) [16, 17], and dual specificity tyrosine-phosphorylation-regulated kinase 1B (mirk/Dyrk1b) phosphorylate cyclin D1 at T288 [18, 19]. In this study, we investigated whether BZN affects cell cycle progression through p38-mediated regulation of cyclin D1 protein phosphorylation and degradation in lung cancer cells.

Materials and methods

Cell lines and drugs

The human lung cancer cell lines A549 and H1299 (ATCC, Rockville, MD, USA) were cultured in DMEM medium (Life Technologies, Gaithersburg, MD, USA) with 10% fetal bovine serum (FBS; Life Technologies) at 37°C in 5% CO_2. Benzethonium chloride, cycloheximide and MG132 obtained from Selleck Chemicals (Huston, TX, USA), and Gefitinib (Cayman Chemicals, Ann Arbor, MI, USA) were dissolved in dimethyl sulfoxide (DMSO).

WST-1 assay

Cell viability was measured using WST-1 assay (Beyotime, Jiangsu, China) as described previously [20]. Cells were seeded in 96-well plates and treated with indicated drugs at various concentrations for different time point. WST-1 was added and incubated at 37°C for 2 h, and then absorbance was read on an automated microplate spectrophotometer (BioTek Instruments, Vermont, USA) at 450 nm.

Colony formation assay

Colony formation assay was performed as described previously [21]. Cells were seeded in 6-well plates and cultured with BZN (up to 20 μM) for 14 days. After washing and fixation, the cells were stained with 1% crystal violet for 5 min. All statistical data were acquired from three independent experiments.

Annexin V-FITC/PI staining assay

Cells were treated with BZN (up to 20 μM) for 48 h, and the cell apoptosis was measured by using Annexin V-FITC/PI Apoptosis Detection Kit (KeyGen, Jiangsu, USA) [22]. Cells were suspended in binding buffer, stained with Annexin V-FITC and PI for 15 min at room temperature in dark. Apoptotic cells were analyzed using a BD Accuri C6 Analyzer (BD Biosciences, San Diego, CA, USA).

Flow cytometric cell cycle analysis

Cells were treated with BZN (up to 20 μM) for 48 h and the cell cycle was determined as described previously [23]. In brief, the cells were fixed and stained with propidium iodide (PI) staining buffer for 10 min at room temperature in dark. Cell cycle distribution was measured using a BD Accuri C6 Analyzer.

Western blot and immunoprecipitation

The whole cell lysates were prepared in lysis buffer (Cell Signaling Technology, Beverly, MA,

USA). The BCA kit (Thermo Fisher Scientific, Waltham, MA, USA) was used to determine the protein concentration. The samples were loaded onto sodium dodecyl sulfate (SDS)-polyacrylamide gel electrophoresis and subsequently electrotransferred to a PVDF membrane (Millipore, Bedford, MA, USA). After blocking with 5% nonfat milk for 1 h, the membrane was incubated with primary antibodies for 2 h at room temperature and washed three times for 10 min each with 1x Tris Buffered Saline with Tween (TBST). And then the membrane was incubated with the corresponding horseradish peroxidase (HRP)-conjugated secondary antibodies for 1 h at room temperature. The reaction was visualized using Clarity Western ECL substrate (Bio-Rad, Hercules, CA, USA) and detected by exposure to autoradiographic film [24]. For immunoprecipitation assay, the detailed experimental procedure was described previously [25].

SILAC labeling and LC-MS/MS analysis

SILAC labeling was described previously [21, 26]. The 'light' labeled A549 cells were treated with 10 μM BZN for 48 h, and the 'heavy' labeled A549 cells were treated with DMSO. A total of 500 μg 'heavy' and 500 μg 'light' proteins were mixed together, and protein digestion and MS analysis were performed as previously described [20]. Peptides were analyzed in Obitrap Fusion Lumos Tribird Mass Specutrometer (Thermo Fisher Scientific) according to the manufacturer's instructions.

Tumorigenicity in nude mice

Female BALB/c nude mice aged 6-8 weeks were maintained under standard conditions and cared for according to the institutional guidelines for animal care. All the animal experiments were approved by the Ethics Committee for Animal Experiments of Jinan University. The study was performed in accordance with the Declaration of Helsinki. A549 cells in equal volumes of PBS and Matrigel were subcutaneously injected into the flanks of mice to establish tumor xenografts [27]. When the tumor xenografts reached 5 mm in diameter, the mice were randomly divided into treatment and control groups. The treatment groups received oral gavage of BZN (10 mg/kg) or intraperitoneal injection of BZN (5 mg/kg) every two days, whereas the control group received vehicle only. The body weight and tumor size was measured every two days, and the tumor volume was calculated using the following equation: $V = (\text{length} \times \text{width}^2)/2$. At the end of the study, tumors, lungs, livers, and kidneys were collected [28]. Proliferative index was determined by immunohistochemistry with the use of Ki-67 antibody (Dako Diagnostics, Mississauga, ON, USA) [29].

Statistical analysis

All *in vitro* experiments were performed in triplicate on three independent experiments. All values were expressed as the means ± SD, and compared using Student's *t*-test. $P < 0.05$ was considered statistically significant.

Results

Identification of potential anticancer drug with a FDA-approved drug library

To screen novel anticancer compounds among the conventional drugs which have been used for other diseases, we took advantage of a compound library comprising of 528 FDA-approved drugs. A549 cells were treated with the 528 compounds or DMSO control for 48 h, and the cell viability was monitored to determine the effect of various drugs on NSCLC cell proliferation (**Figure 1A**). As displayed in **Figure 1A**, a total of 11 drugs exerted an obviously inhibitory effect (> 50%) on cancer cell growth (Table S1), including Epirubicin HCl and Fludarabine, the commonly used drugs for cancer treatment in clinic [30-33], suggesting that our screening strategy could be used to identify novel compounds with anticancer effects. Among the 11 candidates, BZN (**Figure 1B**), a well-known surface antifungal and antibacterial compound [8], which has not been linked to lung cancer treatment, attracted our interest for further study.

Benzethonium chloride inhibits lung cancer cell proliferation

To study the anti-proliferation effect of BZN on lung cancer cells, A549 and H1299 cells were treated with various concentrations of BZN for up to 72 h. As shown in **Figure 1C**, BZN markedly suppressed the cell viability in dose- and time-dependent manners. Moreover, we conducted colony formation assay to further deter-

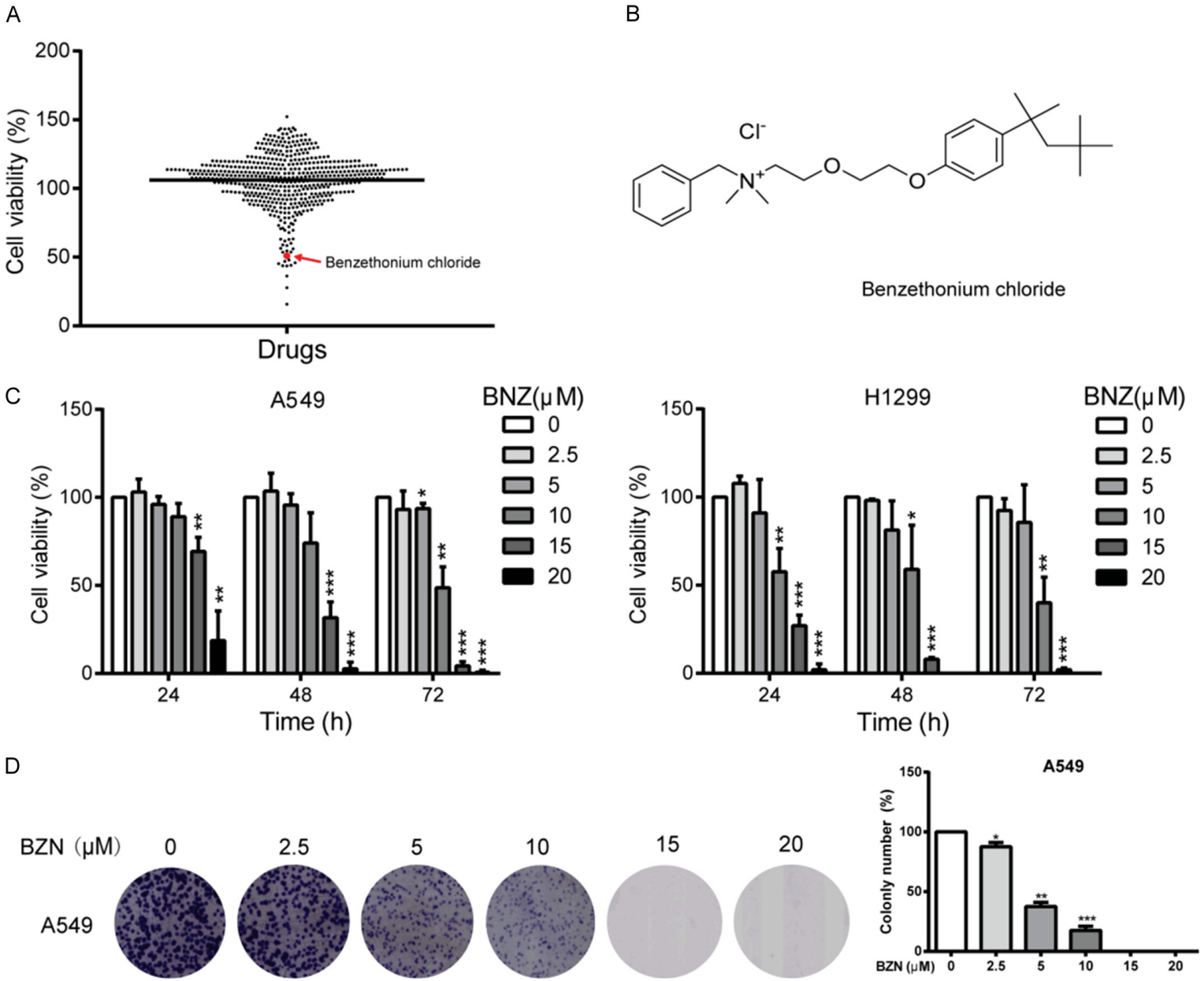
A
Cell viability (%)
200
150
100
50
0
Benzethonium chloride
Drugs
B
Cl-
N+
O
O
Benzethonium chloride
C
A549
BNZ(μM)
0
2.5
5
10
15
20
Cell viability (%)
Time (h)
24
48
72
H1299
D
BZN (μM)
0
2.5
5
10
15
20
A549
Colonly number (%)

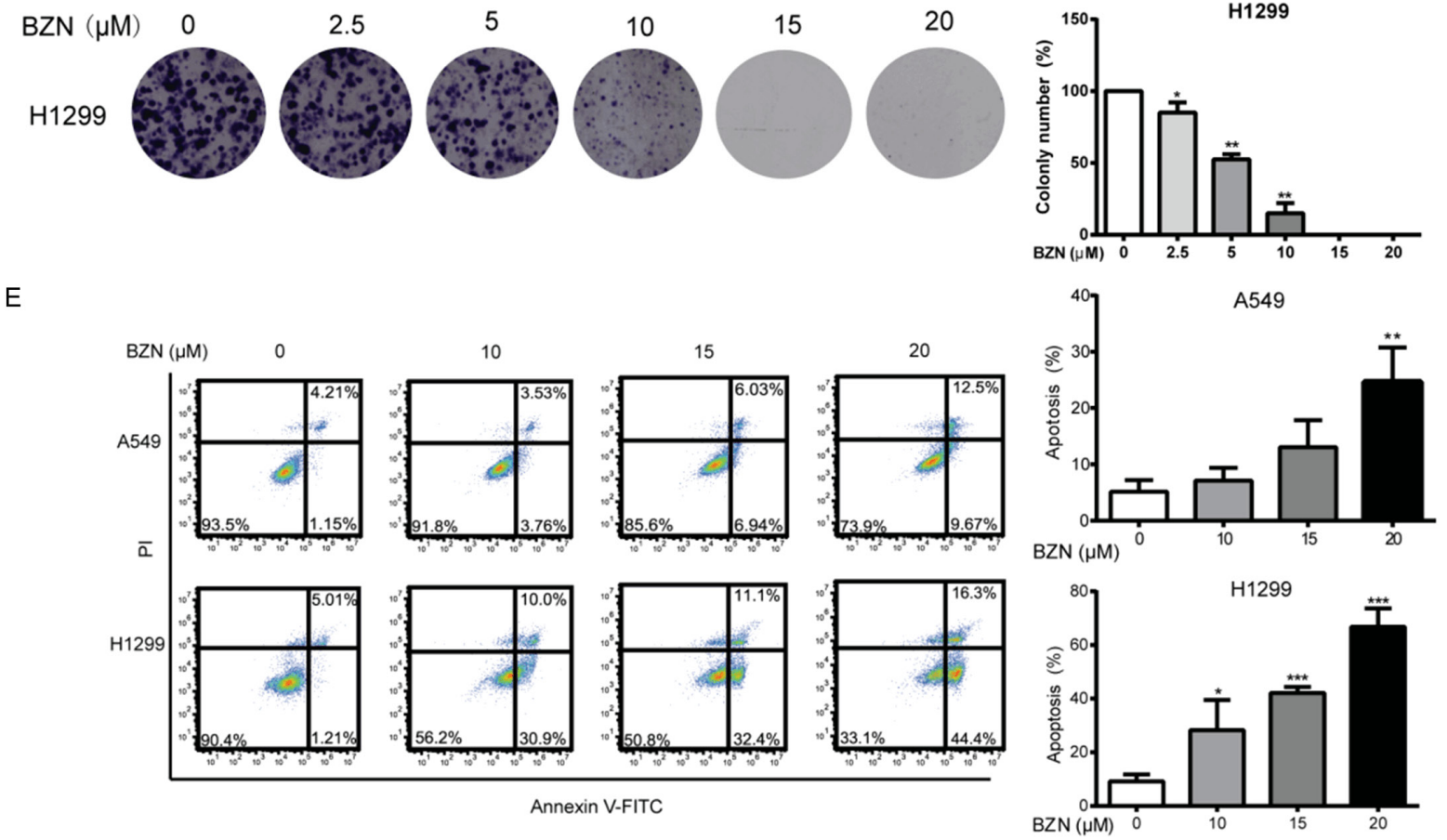

Figure 1. Benzethonium chloride (BZN) inhibites lung cancer cell proliferation. A. A549 cells were treated with the 528 FDA-approved drugs separately, and cell viability was determined by WST-1 assay. B. BZN structure diagram. C. WST-1 assay was performed to detect cell viability in the A549 and H1299 cells treated with different concentrations of BZN for up to 72 h. D. The A549 and H1299 cells treated with BZN (up to 20 μM) were compared for colony formation ability. E. A549 and H1299 were treated with BZN (up to 20 μM) for 48 h, and apoptotic cells were detected by flow cytometry. Note that BZN significantly increased the percentage of apoptotic cells in a dose-dependent manner. F. Western blotting was performed to compare expression levels of caspase-3, cleaved caspase-3, PARP and cleaved PARP. Bars, SD; $*P < 0.05$; $**P < 0.01$; $***P < 0.001$ compared with DMSO-treated cells.

mine the effects of BZN on the growth of lung cancer cells. The results showed that BZN significantly reduced colony formation ability of A549 and H1299 cells (**Figure 1D**), indicating that BZN has potently inhibitory effect on lung cancer cell proliferation.

Benzethonium chloride triggers apoptosis in lung cancer cells

We next used Annexin V-FITC/PI double staining assay to detect whether BZN has effect on apoptosis in lung cancer cells. The flow cytometry data showed that the A549 and H1299 cells treated with BZN exerted an increase in percentage of apoptotic cells in a dose-dependent manner (**Figure 1E**). Consistently, increased expressions of cleaved caspase-3 and cleaved PARP, the active form of caspase-3 and PARP, were observed upon BZN treatment in A549 and H1299 cells (**Figure 1F**), confirming that BZN can induce apoptosis to inhibit cell growth in lung cancer cells.

Quantitative proteomics suggests the involvement of cell cycle control in action mechanisms of benzethonium chloride in cancer cells

To gain insights into the mechanism in anticancer effect of BZN, SILAC-based quantitative proteomics was used to identify the differentially expressed proteins in the BZN-treated lung cancer cells. "Light"-labeled and "Heavy"-labeled A549 cells were treated with 10 μM BZN and DMSO for 48 h, respectively, and then lysated and mixed for mass spectrometry (MS) analysis (**Figure 2A**). Here, a total of 5123 proteins were identified and quantified, among which 3010 proteins were all detected in the triplicate samples (**Figure 2B**). A total of 239 proteins were found to be markedly regulated by BZN (fold change ≥ 1.5 and *P*-value ≤ 0.05) (Table S2), including 60 upregulated and 179 downregulated proteins, respectively (**Figure 2C**), which were uploaded to Ingenuity pathway analysis (IPA) for functional characterization of the signaling that the 239 proteins may participate in [34]. The results suggested that cell cycle control ranks first among the predicted top five canonical pathways, with a *p* value of 4.95×10^{-13} (**Figure 2D**). To confirm the prediction, cell cycle distribution was determined in the BZN-treated A549 and H1299 by flow cytometry, and the data showed that BZN induced a significant cell cycle arrest at G1 phase (**Figure 2E**). Collectively, these data indicated that BZN may affect the process of G1 to S transition to inhibit lung cancer tumorigenesis.

Benzethonium chloride accelerates protein degradation of cyclin D1 through ubiquitin-proteasome pathway

To further dissect the molecular mechanisms how BZN induces G1 cell cycle arrest, expression levels of several key regulators of G1 cell cycle were examined by Western blot. As shown in **Figure 3A**, decreased expressions of cyclin D1, cyclin E1, CDK4 and CDK6 were observed. Cyclin D1 is the most sensitive and important cyclin protein in G1 phase, so we focused on the regulation of cyclin D1 by BZN [14, 19].

We next investigated whether BZN could affect protein degradation of cyclin D1. The interaction of cyclin D1 and ubiquitin was compared in the lung cancer cells with or without BZN treatment by immunoprecipitation, and a significant increase in the binding of ubiquitin to cyclin D1 was observed in both A549 and H1299 cells (**Figure 3B**), suggesting enhanced protein degradation of cyclin D1 upon BZN treatment. Moreover, following a 12 h pretreatment with cycloheximide (CHX), which could inhibit protein synthesis, the cells were exposed to 10 μM BZN. The cell lysates were collected at the indicated time points and compared for cyclin D1 expression using Western blotting. As shown in **Figure 3C**, cyclin D1 protein degradation was accelerated in the BZN-treated lung cancer cells compared with the control cells, suggesting that exposure of cancer cells to BZN leads to degradation of BZN protein. Furthermore, the inhibitory effect of BZN on cyclin D1 expression could be rescued by a proteasome inhibitor MG132 (**Figure 3D**), which strongly supports that BZN induces G1 cell cycle arrest through promoting ubiquitin-mediated proteasomal degradation of cyclin D1.

Benzethonium chloride activates p38 signaling to phosphorylate cyclin D1 at T286

The threonine residue 286 and 288 of cyclin D1 are the key points about the stability. p38 and ERK2 have also been known to regulate cyclin D1 stability by phosphorylating T286, and the phosphorylation of T288 was regulated

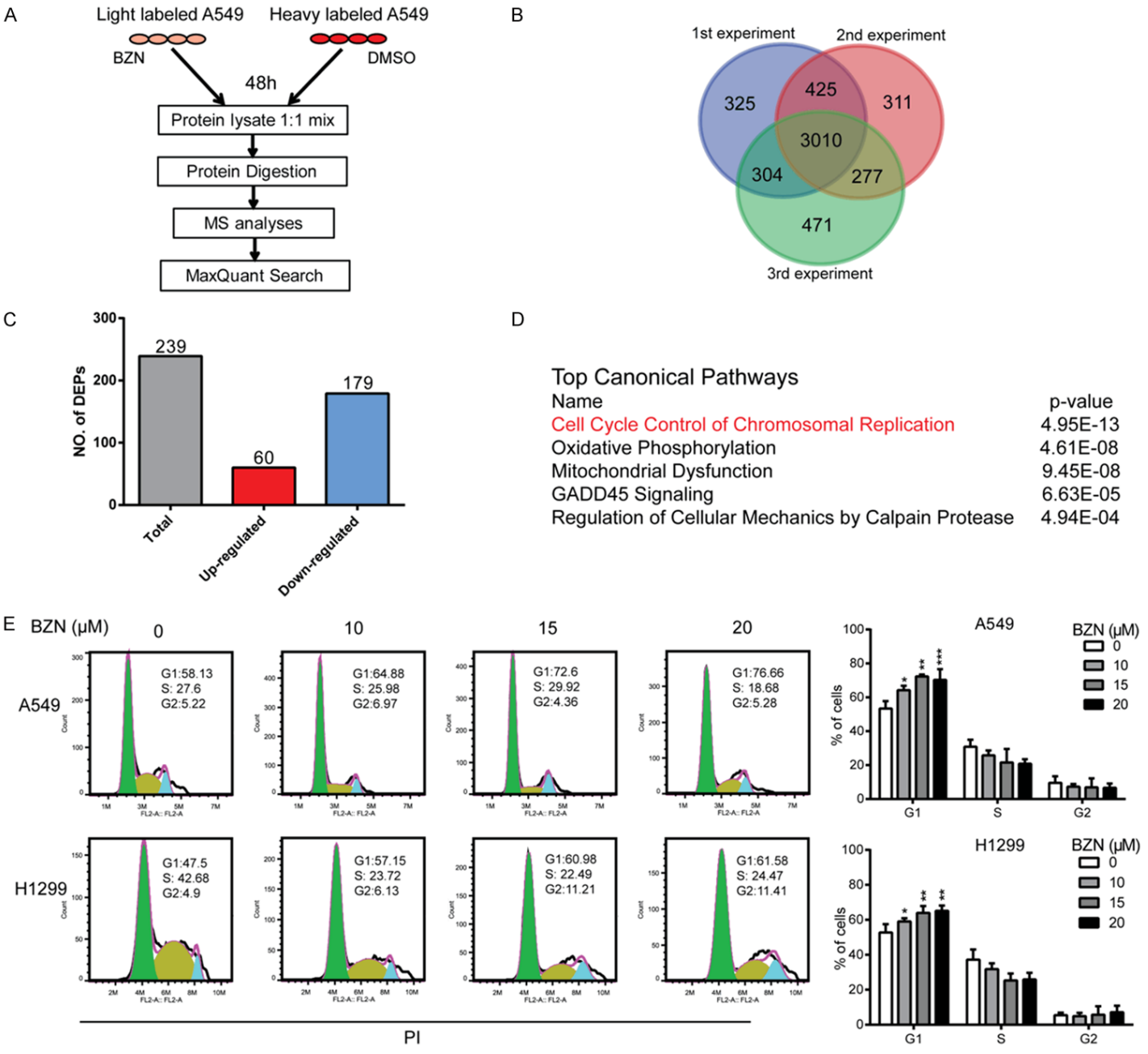
A
Light labeled A549
Heavy labeled A549
BZN
DMSO
48h
Protein lysate 1:1 mix
Protein Digestion
MS analyses
MaxQuant Search
B
1st experiment
2nd experiment
3rd experiment
325
425
311
3010
304
277
471
C
NO. of DEPs
300
200
100
0
239
60
179
Total
Up-regulated
Down-regulated
D
Top Canonical Pathways
Name
p-value
Cell Cycle Control of Chromosomal Replication
4.95E-13
Oxidative Phosphorylation
4.61E-08
Mitochondrial Dysfunction
9.45E-08
GADD45 Signaling
6.63E-05
Regulation of Cellular Mechanics by Calpain Protease
4.94E-04
E
BZN (μM)
0
10
15
20
A549
G1:58.13
S: 27.6
G2:5.22
G1:64.88
S: 25.98
G2:6.97
G1:72.6
S: 29.92
G2:4.36
G1:76.66
S: 18.68
G2:5.28
H1299
G1:47.5
S: 42.68
G2:4.9
G1:57.15
S: 23.72
G2:6.13
G1:60.98
S: 22.49
G2:11.21
G1:61.58
S: 24.47
G2:11.41
PI
% of cells
G1
S
G2

Figure 2. Quantitative proteomics suggests the involvement of cell cycle control in action mechanisms of benzethonium chloride in cancer cells. A. Experimental process of the identification of BZN-regulated proteins by SILAC-based quantitative proteomics experiment. B. Venn diagram showing the identification of overlapped proteins in three biological replicates. C. Differentially expressed proteins with fold change ≥ 1.5 and $P \leq 0.05$ in the BZN-treated A549 cells. D. The top five canonical pathways from the IPA analysis of the differentially expressed proteins in BZN-treated cells. E. A549 and H1299 cells were treated with BZN (up to 20 μM) for 48 h, and cell cycle distribution was analyzed by flow cytometry. Note that BZN arrested cells at G1 phase. Bars, SD; *P < 0.05; **P < 0.01; ***P < 0.001 compared with DMSO-treated cells.

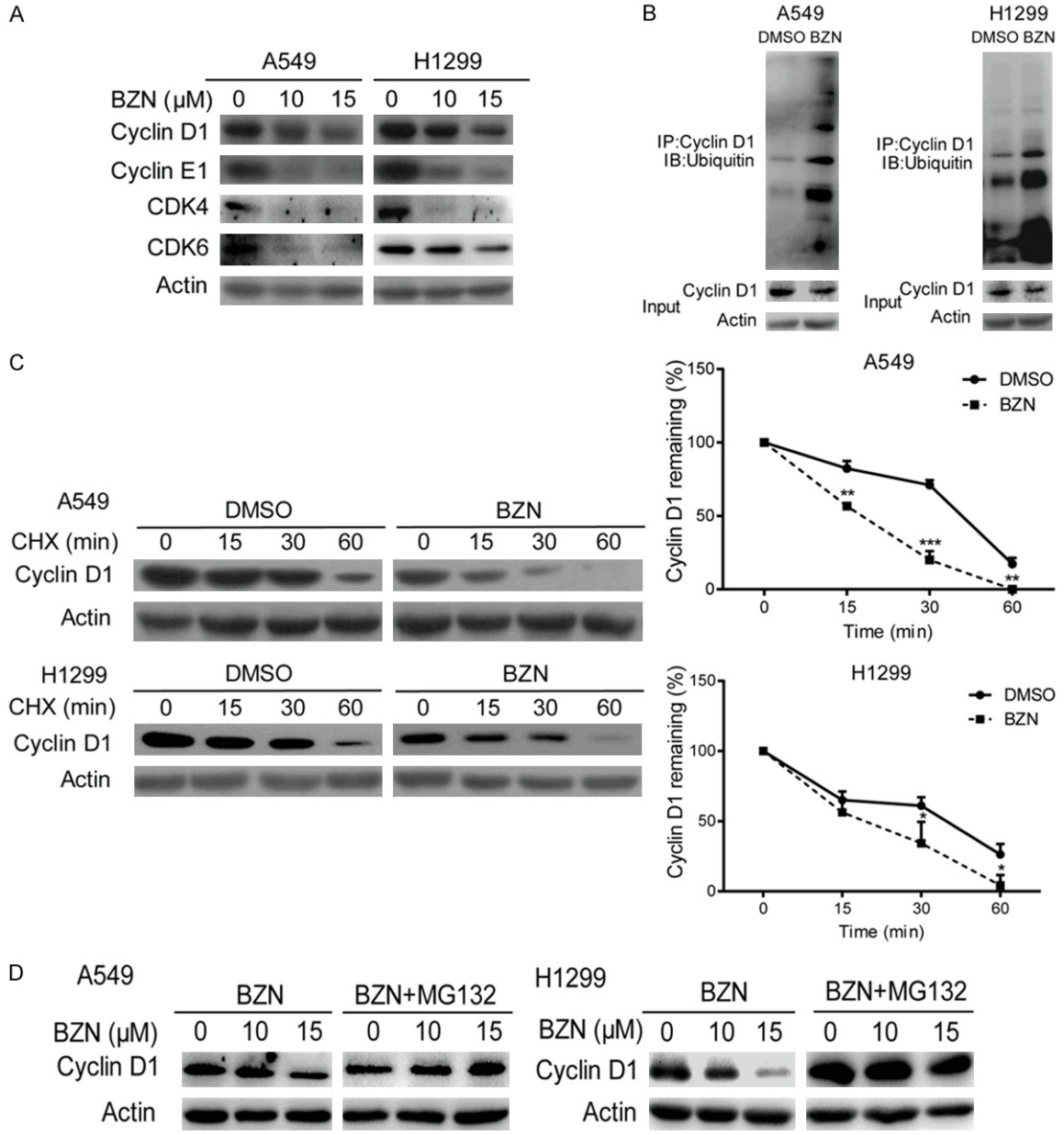

Figure 3. Benzethonium chloride accelerates protein degradation of cyclin D1 through ubiquitin-proteasome pathway. A. Expression levels of the G1 phase specific cyclin and CDK proteins were compared in BZN-treated A549 and H1299 cells by western blot. B. Immunoprecipitation assay was performed in the BZN-treated lung cancer cells, and ubiquitin expression was examined in the cyclin D1 immunoprecipitates. C. After pretreatment with cycloheximide (CHX; 50 μg/mL) for 12 h, A549 and H1299 cells were exposed to 10 μM BZN, and the cell lysates were collected at the indicated time points and compared for cyclin D1 expression using Western blotting. Cyclin D1 signals were quantified by densitometry, and the degradation rate was shown as the ratio of cyclin D1 level at each time point to the respective original level (0 min). D. MG132 could rescue the inhibitory effect of BZN on cyclin D1 expression. Bars, SD; *P < 0.05; **P < 0.01; ***P < 0.001 compared with DMSO-treated cells.

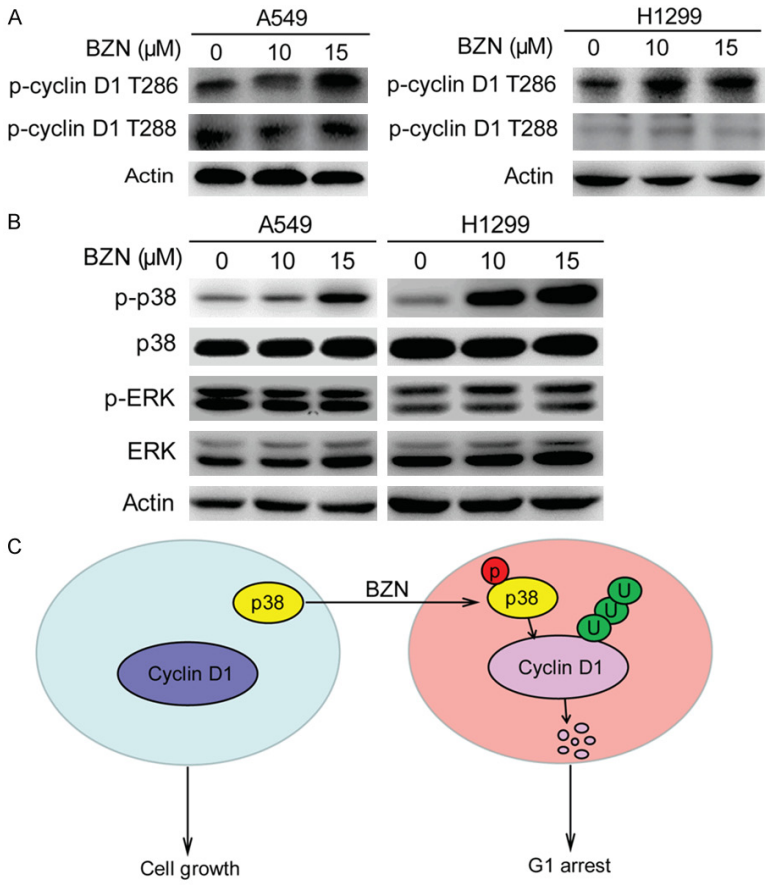

Figure 4. Benzethonium chloride activates p38 signaling to phosphorylate cyclin D1 at T286. A. Comparison of p-cyclin D1 T286 and p-cyclin D1 T288 expression in the BZN-treated A549 and H1299 cells. B. BZN markedly increased p-p38, but did not change p-ERK. C. Schematic diagram summarizing the mechanisms how BZN inhibits lung cancer cell proliferation.

by mirk/Dyrk1b [16, 17]. Therefore, we examined the phosphorylation of T286 and T288 residue after BZN treatment, and the data showed that the phosphorylation of T286 was increased but there was no change in T288 phosphorylation (**Figure 4A**). Since phosphorylation of p38, but not ERK2, was significantly regulated in the BZN-treated lung cancer cells (**Figure 4B**), these observations suggested that BZN could increase ubiquitination degradation of cyclin D1 through activated p38 to phosphorylation T286, thereby inhibiting the growth of lung cancer cells (**Figure 4C**).

Benzethonium chloride sensitizes lung cancer cells to gefitinib

Given that BZN induces G1 cell cycle arrest, we postulated that it could be used as a drug sensitizer in cancer treatment. Gefitinib is a famous standard-of-care treatment in NSCLC patients with EGFR mutations [35, 36]. Unfortunately, most patients inevitably recur due to drug resistance [35, 37, 38]. Here, we detected whether combing BZN with gefitinib could have a synergistic effect to improve treatment efficacy. As shown in **Figure 5A**, although low dose of BZN or gefitinib alone has no or modest effect on cell viability in lung cancer cells, a combination of BZN and gefitinib exerted stronger inhibitory effect on lung cancer cell proliferation, whereas the same conclusion was obtained in colony formation assay (**Figure 5B**). Moreover, the combination of low dose BZN and gefitinib could significantly induce apoptosis in lung cancer cells, compared with the cells treated with BZN or gefitinib alone (**Figure 5C**). Together, BZN can enhance the sensitivity of lung cancer cells to gefitinib.

Benzethonium chloride suppresses the tumor growth in vivo

We next evaluated the therapeutic potential of BZN in nude mice. BZN was intraperitoneally injected or orally administrated to the nude mice bearing subcutaneous tumor xenografts, and tumor volume and body weight of mice were monitored. The results showed that the tumor growth was markedly suppressed by BZN treatment (**Figure 6A** and **6B**). The Ki-67 proliferation index in the tumor xenografts was determined, and the results revealed that BZN inhibited tumor growth via decreased cell proliferation (**Figure 6C**). As shown in **Figure 6D**, western blot analysis indicated that the expression of p-p38, p-Cyclin D1 and cleaved caspase-3 were up-regulated in the tumor xenograft treated with BZN (**Figure 6D**), which was consistent with *in vitro* experiments. In addition, the weight of mice was no significant change between the treatment and control

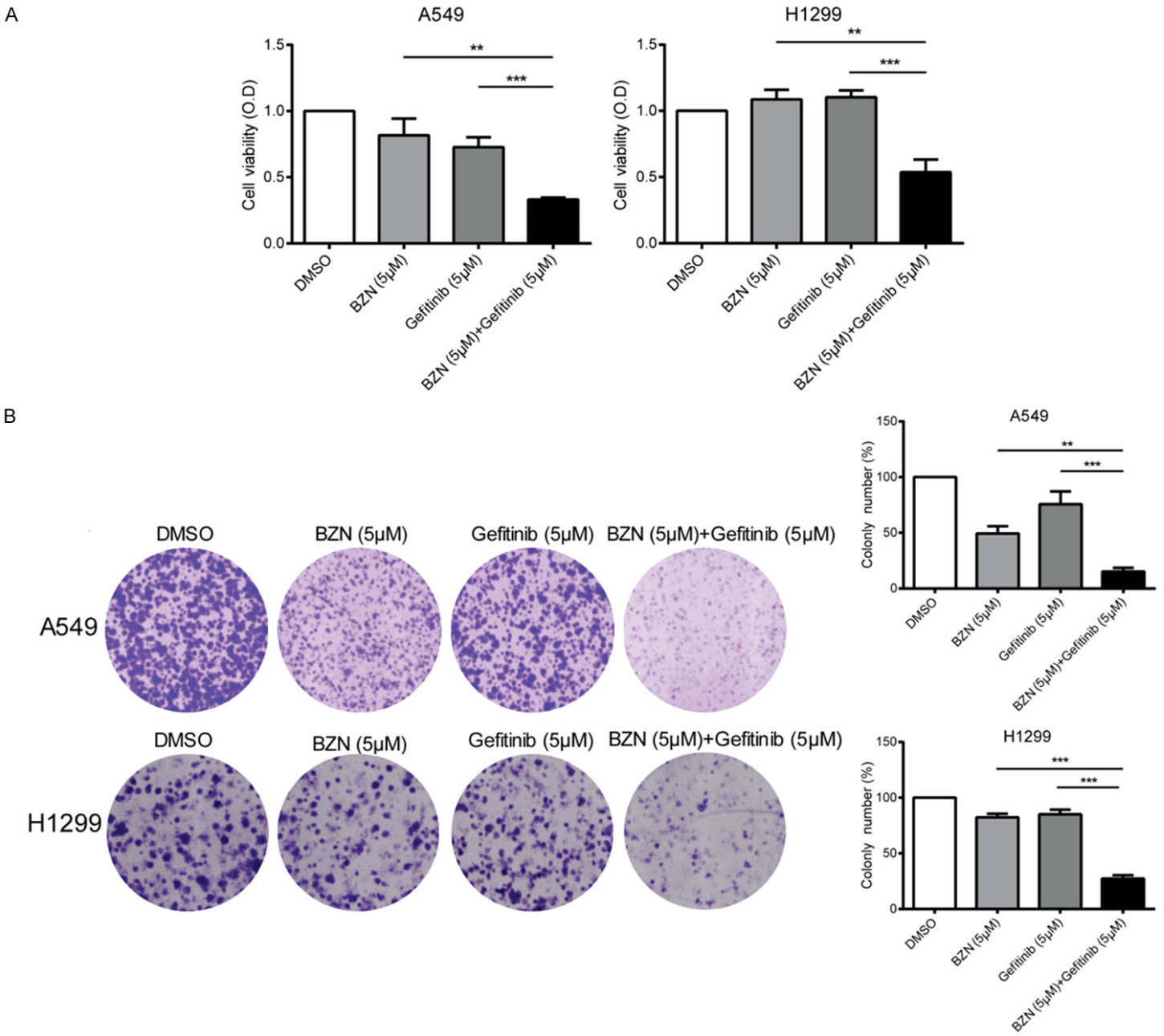
A
A549
H1299
Cell viability (O.D)
1.5
1.0
0.5
0.0
**
***
DMSO
BZN (5μM)
Gefitinib (5μM)
BZN (5μM)+Gefitinib (5μM)
B
DMSO
BZN (5μM)
Gefitinib (5μM)
BZN (5μM)+Gefitinib (5μM)
A549
H1299
Colonly number (%)
150
100
50
0

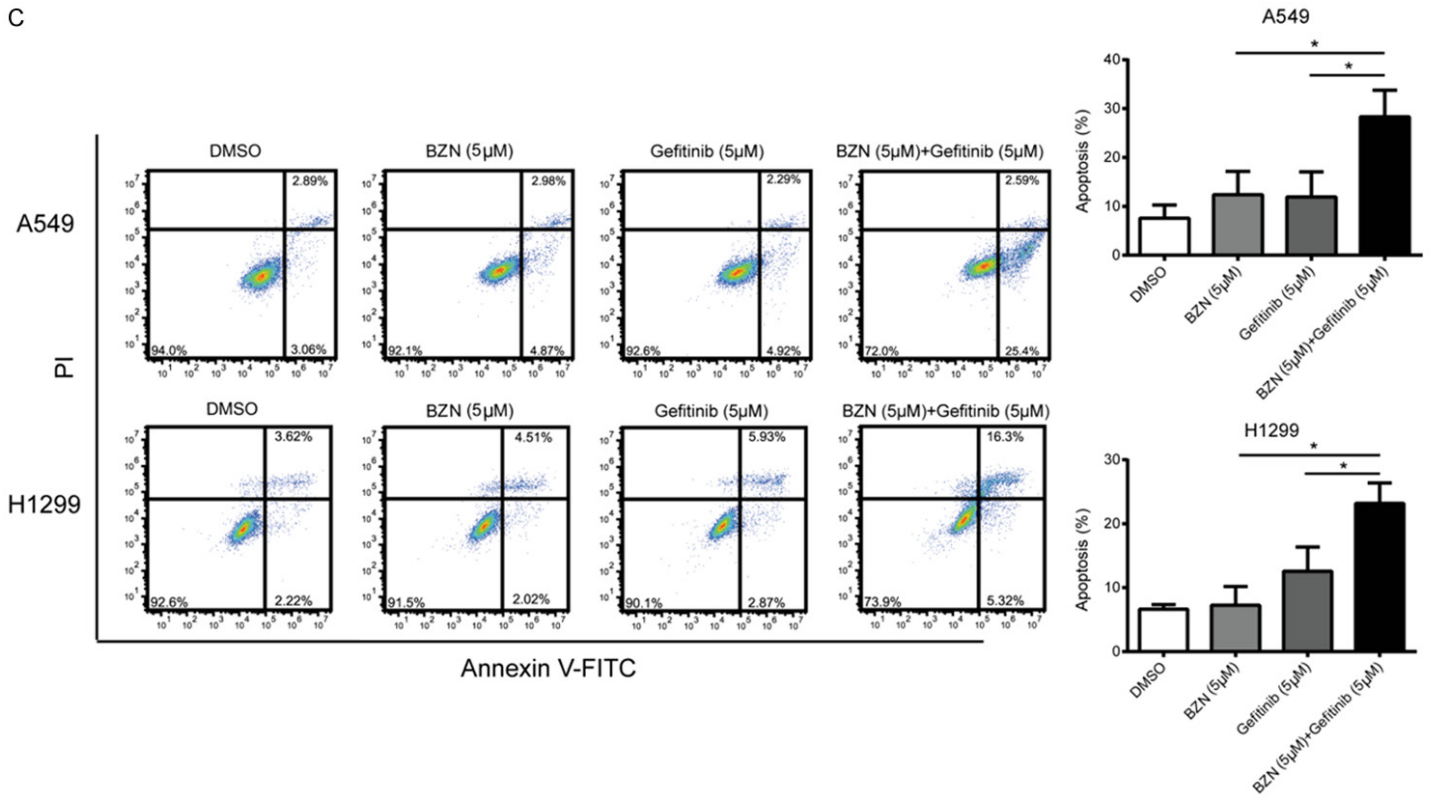

Figure 5. Benzethonium chloride sensitizes lung cancer cells to gefitinib. A. A549 and H1299 were treated with DMSO, BZN (5 μM), Gefitinib (5 μM) or combination of BZN and gefitinib, respectively, for 72 h, and cell viability was determined by WST-1 assay. B. Colony formation assay showed that BZN significantly enhanced the sensitivity of lung cancer cells to gefitinib. C. The percentage of apoptotic cells was detected in the cells treated with DMSO, BZN, gefitinib or the combination. Bars, SD; **P* < 0.05; **P < 0.01; ****P* < 0.001 compared with gefitinib-treated cells.

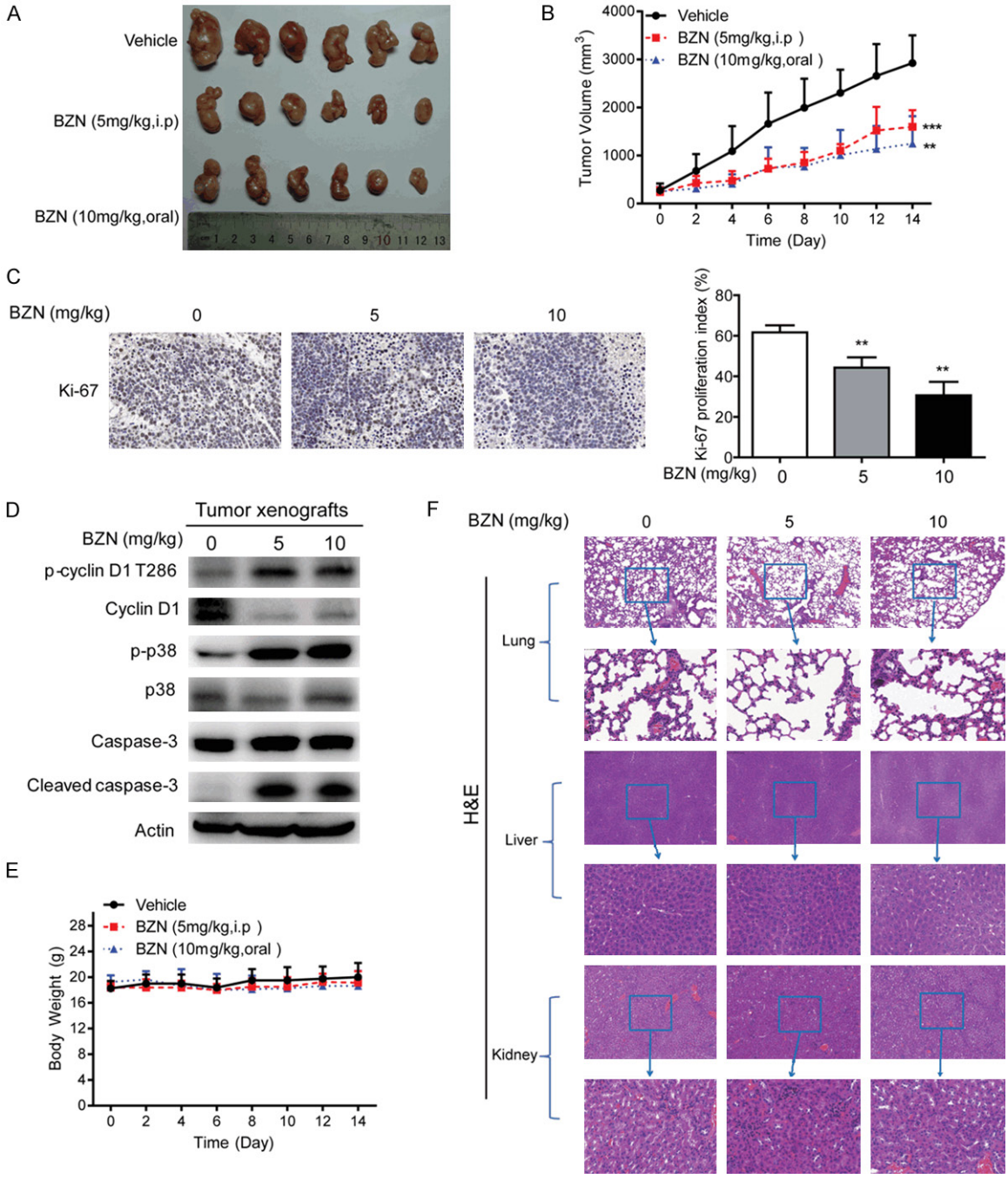

Figure 6. Benzethonium chloride suppresses lung cancer tumorigenesis *in vivo*. A549 cells were subcutaneously injected into nude mice to establish tumor xenograft. When tumor reached ~0.5 cm diameter, the mice were randomized into three groups to receive oral gavage of BZN (10 mg/kg), intraperitoneal injection of BZN (5 mg/kg) or vehicle control every two days, respectively. A. Image of tumors in control group and BZN treatment groups. B. Tumor curves showing the suppressive effect of BZN on growth of A549-derived tumor xenografts (n = 6). C. Immunohistochemical analysis of Ki-67 proliferation index in tumor xenografts treated with BZN and vehicle. D. Western blot was performed to compare expression levels of p-cyclin D1 T286, cyclin D1, p-p38, p38, caspase-3 and cleaved caspase-3 in the tumor xenograft treated with BZN and vehicle, respectively. E. Body weight of nude mice during the experimental period. F. Hematoxylin and eosin (H&E) staining of the lungs, livers and kidneys collected from treatment and control groups. Bars, SD; $^{**}P < 0.01$; $^{***}P < 0.001$ compared with control group.

groups (**Figure 6E**). Histological examination of vital organs, including lungs, livers and kidneys, did not reveal any overt changes in morphology (**Figure 6F**). These data suggested that BZN

could inhibit the tumor growth and with low toxicity *in vivo*.

Discussion

The discovery of new drugs is a long process that requires high investment but faces various unknown risks. Since the clinical drug development success rate is very low in recent years, there is an emerging recognition that identification of new indications for the existing drugs could be a relatively low-cost and efficient strategy for development of novel anticancer reagents [39]. Mifepristone (MIF), a drug regularly used for abortion, has been reported to have anti-tumor activity in multiple hormone-dependent cancers, including luminal type breast cancer [40]. Celecoxib, a drug for rheumatoid arthritis, has been reported to suppress cutaneous squamous cell carcinoma cell (CSCC) migration [41]. In this study, we provide the first evidence that BZN, a FDA-approved drug for anti-infective products, induces apoptosis and suppresses proliferation and tumorigenesis of lung cancer. Actually, our findings were corroborated by the recent studies that BZN can activate endoplasmic reticulum (ER) stress and reduce proliferation in head and neck cancer (HNSCC) [8]. The National Cancer Institute/NIH Developmental Therapeutics Program on 60 human cancer cell lines revealed that BZN has broad-range antitumor activity [42]. However, there was no related research about the use of BZN in lung cancer. Our study here suggests that BZN could be a promising therapeutic agent in lung cancer treatment.

Increasing therapeutic agents have been identified to induce cyclin D1 degradation *in vitro* [43, 44]. Cyclin D1 is a critical regulator of cell cycle progression. Together with its binding partners CDK4 and CDK6, cyclin D1 form active complexes that promote G1 to S phase transition by phosphorylating and inactivating the Rb [45]. Overexpression of cyclin D1 is frequently observed in various cancers and correlates to cancer development and progression. Cyclin D1 is a very unstable protein with a short half-life, indicating that enhancement of cyclin D1 protein degradation may offer a useful strategy for therapeutic intervention. Previous report suggests that knockdown of ubiquitin-specific proteases 2 (USP2), a specific deubiquitinase to stabilize cyclin D1, can destablize cyclin D1 and induce growth arrest in human cancer cells [46]. In addition, the ablation of cyclin D1 can shut off the growth of human breast cancers with activated Neu-Ras pathway [46, 47]. In this study, we demonstrated that BZN can suppress lung cancer tumorigenesis. Mechanistically, BZN treatment activates p38 signaling to phosphorylate cyclin D1 at T286 and enhances the interaction between ubiquitin and cyclin D1, therefore promoting cyclin D1 degradation to induce cell cycle arrest and inhibit cancer cell proliferation. Our findings here further support solid evidence on the rationale of cyclin D1 as a therapeutic target in cancer treatment.

Lung cancer is a deadly disease with the highest lethality rate among all cancers. Overexpression or mutations of epidermal growth factor receptor (EGFR) is largely responsible for development and progression of NSCLC [48]. Gefitinib, a tyrosine kinase inhibitor (TKI), has been shown to significantly improve the prognosis of patients and extensively used as the first line therapy in advanced NSCLC patients with EGFR mutations [49]. Unfortunately, most patients inevitably relapse because of resistance [50]. Therefore, it is urgent to improve efficacy of gefitinib treatment. In this study, we found that the combination of BZN and gefitinib significantly induced apoptosis and exerted stronger inhibitory effects on cell proliferation in lung cancer cells (**Figure 5**). Our results imply that BZN is a promising medicine to improve gefitinib efficacy in NSCLC.

Acknowledgements

The work was supported by the National Key R & D Program of China (2017YFA0505100), The National Natural Science Foundation of China (31570828, 31770888, 81803551, 81773-085) and Guangdong Natural Science Research Grant (2016A030313838).

Disclosure of conflict of interest

None.

Address correspondence to: Qing-Yu He and Dr. Bin Li, Institute of Life and Health Engineering, College of Life Science and Technology, Jinan University, Guangzhou 510632, China. Tel: +86-20-85227039; Fax: +86-20-85227039; E-mail: tqyhe@email.jnu.edu.cn (QYH); Tel: +86-20-85224372; Fax: +86-20-85224372; E-mail: libin2015@jnu.edu.cn (BL)

References

[1] Bray F, Ferlay J, Soerjomataram I, Siegel RL, Torre LA and Jemal A. Global cancer statistics 2018: GLOBOCAN estimates of incidence and mortality worldwide for 36 cancers in 185 countries. CA Cancer J Clin 2018; 68: 394-424.

[2] Ferlay J, Colombet M, Soerjomataram I, Mathers C, Parkin DM, Pineros M, Znaor A and Bray F. Estimating the global cancer incidence and mortality in 2018: GLOBOCAN sources and methods. Int J Cancer 2019; 144: 1941-1953.

[3] Njatcha C, Farooqui M, Kornberg A, Johnson DE, Grandis JR and Siegfried JM. STAT3 cyclic decoy demonstrates robust antitumor effects in non-small cell lung cancer. Mol Cancer Ther 2018; 17: 1917-1926.

[4] Li LJ, Chen DF, Wu GF, Guan WJ, Zhu Z, Liu YQ, Gao GY, Qin YY and Zhong NS. Incidence and risk of thromboembolism associated with bevacizumab in patients with non-small cell lung carcinoma. J Thorac Dis 2018; 10: 5010-5022.

[5] Wang H, Zhang X, Vidaurre I, Cai R, Sha W and Schally AV. Inhibition of experimental small-cell and non-small-cell lung cancers by novel antagonists of growth hormone-releasing hormone. Int J Cancer 2018; 142: 2394-2404.

[6] Spiro SG and Silvestri GA. One hundred years of lung cancer. Am J Respir Crit Care Med 2005; 172: 523-529.

[7] Skrott Z, Mistrik M, Andersen KK, Friis S, Majera D, Gursky J, Ozdian T, Bartkova J, Turi Z, Moudry P, Kraus M, Michalova M, Vaclavkova J, Dzubak P, Vrobel I, Pouckova P, Sedlacek J, Miklovicova A, Kutt A, Li J, Mattova J, Driessen C, Dou QP, Olsen J, Hajduch M, Cvek B, Deshaies RJ and Bartek J. Alcohol-abuse drug disulfiram targets cancer via p97 segregase adaptor NPL4. Nature 2017; 552: 194-199.

[8] Rayess HM, Xi Y, Garshott DM, Brownell AL, Yoo GH, Callaghan MU and Fribley AM. Benzethonium chloride activates ER stress and reduces proliferation in HNSCC. Oral Oncol 2018; 76: 27-33.

[9] Wang Y, Li YJ, Huang XH, Zheng CC, Yin XF, Li B and He QY. Liensinine perchlorate inhibits colorectal cancer tumorigenesis by inducing mitochondrial dysfunction and apoptosis. Food Funct 2018; 9: 5536-5546.

[10] Xu WW, Zheng CC, Huang YN, Chen WY, Yang QS, Ren JY, Wang YM, He QY, Liao HX and Li B. Synephrine hydrochloride suppresses esophageal cancer tumor growth and metastatic potential through inhibition of Galectin-3-AKT/ERK signaling. J Agric Food Chem 2018; 66: 9248-9258.

[11] Xu H, Dephoure N, Sun H, Zhang H, Fan F, Liu J, Ning X, Dai S, Liu B, Gao M, Fu S, Gygi SP and Zhou C. Proteomic profiling of paclitaxel treated cells identifies a novel mechanism of drug resistance mediated by PDCD4. J Proteome Res 2015; 14: 2480-2491.

[12] McKay JA, Douglas JJ, Ross VG, Curran S, Murray GI, Cassidy J and McLeod HL. Cyclin D1 protein expression and gene polymorphism in colorectal cancer. Aberdeen colorectal initiative. Int J Cancer 2000; 88: 77-81.

[13] Santra MK, Wajapeyee N and Green MR. F-box protein FBX031 mediates cyclin D1 degradation to induce G1 arrest after DNA damage. Nature 2009; 459: 722-725.

[14] Lee JT, Shan J and Gu W. Targeting the degradation of cyclin D1 will help to eliminate oncogene addiction. Cell Cycle 2010; 9: 857-858.

[15] Knudsen KE, Diehl JA, Haiman CA and Knudsen ES. Cyclin D1: polymorphism, aberrant splicing and cancer risk. Oncogene 2006; 25: 1620-1628.

[16] Okabe H, Lee SH, Phuchareon J, Albertson DG, McCormick F and Tetsu O. A critical role for FBXW8 and MAPK in cyclin D1 degradation and cancer cell proliferation. PLoS One 2006; 1: e128.

[17] Diehl JA, Zindy F and Sherr CJ. Inhibition of cyclin D1 phosphorylation on threonine-286 prevents its rapid degradation via the ubiquitin-proteasome pathway. Genes Dev 1997; 11: 957-972.

[18] Zou Y, Ewton DZ, Deng X, Mercer SE and Friedman E. Mirk/dyrk1B kinase destabilizes cyclin D1 by phosphorylation at threonine 288. J Biol Chem 2004; 279: 27790-27798.

[19] Alao JP. The regulation of cyclin D1 degradation: roles in cancer development and the potential for therapeutic invention. Mol Cancer 2007; 6: 24.

[20] Wang Y, Yu RY, Zhang J, Zhang WX, Huang ZH, Hu HF, Li YL, Li B and He QY. Inhibition of Nrf2 enhances the anticancer effect of 6-O-angeloylenolin in lung adenocarcinoma. Biochem Pharmacol 2017; 129: 43-53.

[21] Wang Y, Zhang J, Huang ZH, Huang XH, Zheng WB, Yin XF, Li YL, Li B and He QY. Isodeoxyelephantopin induces protective autophagy in lung cancer cells via Nrf2-p62-keap1 feedback loop. Cell Death Dis 2017; 8: e2876.

[22] Zheng WB, Li YJ, Wang Y, Yang J, Zheng CC, Huang XH, Li B and He QY. Propafenone suppresses esophageal cancer proliferation through inducing mitochondrial dysfunction. Am J Cancer Res 2017; 7: 2245-2256.

[23] Zhong Y, Yang J, Xu WW, Wang Y, Zheng CC, Li B and He QY. KCTD12 promotes tumorigenesis by facilitating CDC25B/CDK1/Aurora A-dependent G2/M transition. Oncogene 2017; 36: 6177-6189.

[24] Xu WW, Li B, Zhao JF, Yang JG, Li JQ, Tsao SW, He QY and Cheung ALM. IGF2 induces CD133

expression in esophageal cancer cells to promote cancer stemness. Cancer Lett 2018; 425: 88-100.

[25] Li B, Xu WW, Guan XY, Qin YR, Law S, Lee NP, Chan KT, Tam PY, Li YY, Chan KW, Yuen HF, Tsao SW, He QY and Cheung AL. Competitive binding between Id1 and E2F1 to Cdc20 regulates E2F1 degradation and thymidylate synthase expression to promote esophageal cancer chemoresistance. Clin Cancer Res 2016; 22: 1243-1255.

[26] Hu HF, Xu WW, Wang Y, Zheng CC, Zhang WX, Li B and He QY. Comparative proteomics analysis identifies Cdc42-Cdc42BPA signaling as prognostic biomarker and therapeutic target for colon cancer invasion. J Proteome Res 2018; 17: 265-275.

[27] Xu WW, Li B, Guan XY, Chung SK, Wang Y, Yip YL, Law SY, Chan KT, Lee NP, Chan KW, Xu LY, Li EM, Tsao SW, He QY and Cheung AL. Cancer cell-secreted IGF2 instigates fibroblasts and bone marrow-derived vascular progenitor cells to promote cancer progression. Nat Commun 2017; 8: 14399.

[28] Li B, Xu WW, Han L, Chan KT, Tsao SW, Lee NPY, Law S, Xu LY, Li EM, Chan KW, Qin YR, Guan XY, He QY and Cheung ALM. MicroRNA-377 suppresses initiation and progression of esophageal cancer by inhibiting CD133 and VEGF. Oncogene 2017; 36: 3986-4000.

[29] Li B, Tsao SW, Chan KW, Ludwig DL, Novosyadlyy R, Li YY, He QY and Cheung AL. Id1-induced IGF-II and its autocrine/endocrine promotion of esophageal cancer progression and chemoresistance-implications for IGF-II and IGF-IR-targeted therapy. Clin Cancer Res 2014; 20: 2651-62.

[30] Wu J, Xue X, Zhang B, Cao H, Kong F, Jiang W, Li J, Sun D and Guo R. Enhanced antitumor activity and attenuated cardiotoxicity of epirubicin combined with paeonol against breast cancer. Tumour Biol 2016; 37: 12301-12313.

[31] An L, Li DD, Chu HX, Zhang Q, Wang CL, Fan YH, Song Q, Ma HD, Feng F and Zhao QC. Terfenadine combined with epirubicin impedes the chemo-resistant human non-small cell lung cancer both in vitro and in vivo through EMT and Notch reversal. Pharmacol Res 2017; 124: 105-115.

[32] Nitsche M, Christiansen H, Lederer K, Griesinger F, Schmidberger H and Pradier O. Fludarabine combined with radiotherapy in patients with locally advanced NSCLC lung carcinoma: a phase I study. J Cancer Res Clin Oncol 2012; 138: 1113-1120.

[33] Chow KU, Kim SZ, von Neuhoff N, Schlegelberger B, Stilgenbauer S, Wunderle L, Cordes HJ and Bergmann L. Clinical efficacy of immunochemotherapy with fludarabine, epirubicin and rituximab in the treatment for chronic lymphocytic leukaemia and prolymphocytic leukaemia. Eur J Haematol 2011; 87: 426-433.

[34] Liu WT, Wang Y, Zhang J, Ye F, Huang XH, Li B and He QY. A novel strategy of integrated microarray analysis identifies CENPA, CDK1 and CDC20 as a cluster of diagnostic biomarkers in lung adenocarcinoma. Cancer Lett 2018; 425: 43-53.

[35] Mao J, Ma L, Shen Y, Zhu K, Zhang R, Xi W, Ruan Z, Luo C, Chen Z, Xi X and Chen S. Arsenic circumvents the gefitinib resistance by binding to P62 and mediating autophagic degradation of EGFR in non-small cell lung cancer. Cell Death Dis 2018; 9: 963.

[36] Wang Y, Xie S and He B. Effect of EGFR gene polymorphism on efficacy of chemotherapy combined with targeted therapy for non-small cell lung cancer in Chinese patients. Am J Cancer Res 2019; 9: 619-627.

[37] Yi H, Li S, Li H, Wang P, Zheng H and Cheng X. Gefitinib induces non-small cell lung cancer H1650 cell apoptosis through downregulating tumor necrosis factor-related apoptosis-inducing ligand expression levels. Oncol Lett 2018; 16: 4768-4772.

[38] Tang X, Jiang J, Zhu J, He N and Tan J. HOXA4-regulated miR-138 suppresses proliferation and gefitinib resistance in non-small cell lung cancer. Mol Genet Genomics 2018; 294: 85-93.

[39] Li Y, Li PK, Roberts MJ, Arend RC, Samant RS and Buchsbaum DJ. Multi-targeted therapy of cancer by niclosamide: a new application for an old drug. Cancer Lett 2014; 349: 8-14.

[40] Liu R, Shi P, Nie Z, Liang H, Zhou Z, Chen W, Chen H, Dong C, Yang R, Liu S and Chen C. Mifepristone suppresses basal triple-negative breast cancer stem cells by down-regulating KLF5 expression. Theranostics 2016; 6: 533-544.

[41] Gong T, Yu Y, Yang B, Lin M, Huang JW, Cheng B and Ji C. Celecoxib suppresses cutaneous squamous-cell carcinoma cell migration via inhibition of SDF1-induced endocytosis of CXCR4. Onco Targets Ther 2018; 11: 8063-8071.

[42] Yip KW, Mao X, Au PY, Hedley DW, Chow S, Dalili S, Mocanu JD, Bastianutto C, Schimmer A and Liu FF. Benzethonium chloride: a novel anticancer agent identified by using a cell-based small-molecule screen. Clin Cancer Res 2006; 12: 5557-5569.

[43] Alao JP, Stavropoulou AV, Lam EW, Coombes RC and Vigushin DM. Histone deacetylase inhibitor, trichostatin a induces ubiquitin-depen-

dent cyclin D1 degradation in MCF-7 breast cancer cells. Mol Cancer 2006; 5: 8.
[44] Feng Q, Sekula D, Muller R, Freemantle SJ and Dmitrovsky E. Uncovering residues that regulate cyclin D1 proteasomal degradation. Oncogene 2007; 26: 5098-5106.
[45] Tian XP, Jin XH, Li M, Huang WJ, Xie D and Zhang JX. The depletion of PinX1 involved in the tumorigenesis of non-small cell lung cancer promotes cell proliferation via p15/cyclin D1 pathway. Mol Cancer 2017; 16: 74.
[46] Shan J, Zhao W and Gu W. Suppression of cancer cell growth by promoting cyclin D1 degradation. Mol Cell 2009; 36: 469-476.
[47] Yu Q, Geng Y and Sicinski P. Specific protection against breast cancers by cyclin D1 ablation. Nature 2001; 411: 1017-1021.
[48] Liang S, Lin M, Niu L, Xu K, Wang X, Liang Y, Zhang M, Du D and Chen J. Cetuximab combined with natural killer cells therapy: an alternative to chemoradiotherapy for patients with advanced non-small cell lung cancer (NSCLC). Am J Cancer Res 2018; 8: 879-891.
[49] Lin Y, Wang X and Jin H. EGFR-TKI resistance in NSCLC patients: mechanisms and strategies. Am J Cancer Res 2014; 4: 411-435.
[50] Guerard M, Robin T, Perron P, Hatat AS, David-Boudet L, Vanwonterghem L, Busser B, Coll JL, Lantuejoul S, Eymin B, Hurbin A and Gazzeri S. Nuclear translocation of IGF1R by intracellular amphiregulin contributes to the resistance of lung tumour cells to EGFR-TKI. Cancer Lett 2018; 420: 146-155.

Table S1. The name and inhibitory rate of 11 drug candidates

Drug name	Inhibitory rate	Drug name	Inhibitory rate
Fludarabine Phosphate	54.82%	Disulfiram	56.38%
Epirubicin HCl	55.84%	Crystal Violet	72.24%
Artemisinin	56.16%	Zinc Pyrithione	85.36%
Ispinesib	54.04%	Penfluridol	67.85%
Ponatinib	53.16%	Benzethonium Chloride	51.49%
Fludarabine	52.11		

Table S2. Differentially expressed proteins in the BZN-treated A549 cells

Protein Name	Accession ID	Fold change
PDLIM7	Q9NR12	5.143333
HSPB1	P04792	3.441667
PTGES	O14684	2.546333
SERPINB6	P35237	2.399333
MRC2	Q9UBG0	2.384
STRA6	Q9BX79	2.350667
EEA1	Q15075	2.289667
TGM2	P21980	2.262333
ACSL4	O60488	2.125667
DPP7	Q9UHL4	2.068667
TNFAIP2	Q03169	2.064667
ANXA3	P12429	2.054
LIMCH1	Q9UPQ0	1.984667
VKORC1	Q9BQB6	1.983667
CNN2	Q99439	1.960333
ITGA3	P26006	1.934667
TRIOBP	Q9H2D6	1.932
ALG2	Q9H553	1.926667
CNTN1	Q12860	1.895333
PSAT1	Q9Y617	1.876
FSCN1	Q16658	1.805
ERGIC1	Q969X5	1.798333
H1F0	P07305	1.794667
AHNAK2	Q8IVF2	1.792
DDAH2	O95865	1.788667
LPP	Q93052	1.779333
LGALS3	P17931	1.771333
MT2A	P02795	1.744333
CSRP1	P21291	1.744
AHNAK	Q09666	1.738333
NAV3	Q8IVL0	1.727667
MBOAT7	Q96N66	1.725667
ACO1	P21399	1.725
MYH9	P35579	1.705333
FLNA	P21333	1.694667
FERMT2	Q96AC1	1.693667
MYL12B	O14950	1.692667
GPHN	Q9NQX3	1.660667
LMNA	P02545	1.657333

PYGL	P06737	1.649333
MVP	Q14764	1.648667
HSDL2	Q6YN16	1.638333
ALDH3B1	P43353	1.632667
LACTB	P83111	1.625667
VCL	P18206	1.624333
CALD1	Q05682	1.615
CORO1B	Q9BR76	1.605667
HCCS	P53701	1.6
ANKLE2	Q86XL3	1.59
ACADVL	P49748	1.582
GALNT2	Q10471	1.573667
ATP2C1	P98194	1.565
PLOD3	O60568	1.560667
RAB8B	Q92930	1.531
SEC61A1	P61619	1.524667
PGM1	P36871	1.522667
ENAH	Q8N8S7	1.522
CAVIN1	Q6NZI2	1.519667
VAT1	Q99536	1.514667
SOD2	P04179	1.504667
NDUFC2	O95298	0.67
DDX23	Q9BUQ8	0.669667
LXN	Q9BS40	0.669667
PAIP1	Q9H074	0.667667
ADNP	Q9H2P0	0.667667
UTP4	Q969X6	0.667333
MRPL12	P52815	0.667
SWAP70	Q9UH65	0.664667
HSPA8	P11142	0.660333
TRIM33	Q9UPN9	0.659
ESF1	Q9H501	0.658
RAB3GAP1	Q15042	0.656
SCD	O00767	0.654333
NDUFS3	O75489	0.654
NDUFA7	O95182	0.649667
KIFC3	Q9BVG8	0.646667
INCENP	Q9NQS7	0.645667
WDHD1	O75717	0.642667
ELAC2	Q9BQ52	0.642
EARS2	Q5JPH6	0.636333
GPKOW	Q92917	0.634667
NDUFA2	O43678	0.634333
MCU	Q8NE86	0.634
MBD3	O95983	0.632667
RHPN2	Q8IUC4	0.628
TOP2A	P11388	0.627
CSDE1	O75534	0.626333
NLRP2	Q9NX02	0.626
MRPS7	Q9Y2R9	0.625333

HEXIM1	O94992	0.625333
CSNK2A1	P68400	0.622667
STRAP	Q9Y3F4	0.622333
GPRC5A	Q8NFJ5	0.617
CPSF2	Q9P2I0	0.617
NDUFA5	Q16718	0.617
LIG3	P49916	0.609667
ORC4	O43929	0.606333
SMC4	Q9NTJ3	0.606333
TUSC3	Q13454	0.606333
AKR1B10	O60218	0.606
MRPL49	Q13405	0.605
TTC27	Q6P3X3	0.604
SLC35A4	L0R6Q1	0.602333
RABL6	Q3YEC7	0.601333
DDX21	Q9NR30	0.596333
PNPT1	Q8TCS8	0.596
UBR7	Q8N806	0.596
UTP18	Q9Y5J1	0.593667
MRPL4	Q9BYD3	0.590667
HECTD1	Q9ULT8	0.589333
NDUFA10	O95299	0.587667
HMOX1	P09601	0.587
RRM1	P23921	0.586667
PTCD3	Q96EY7	0.577
BYSL	Q13895	0.576667
NDUFA13	Q9P0J0	0.575667
DDX5	P17844	0.573
NDUFA4	O00483	0.572333
MRPL21	Q7Z2W9	0.572
QSOX2	Q6ZRP7	0.568333
HGD	Q93099	0.567333
TRIP12	Q14669	0.565667
NUDT1	P36639	0.565667
SQSTM1	Q13501	0.564667
MRPL42	Q9Y6G3	0.564333
MRPS9	P82933	0.563
CDK1	P06493	0.561667
KLF16	Q9BXK1	0.561
NDUFS1	P28331	0.560667
SMC2	O95347	0.557
MCM3	P25205	0.556667
PLA2G4A	P47712	0.556
UPF3B	Q9BZI7	0.553667
ALDH3A1	P30838	0.553
MCM7	P33993	0.552333
PC	P11498	0.552
MTPAP	Q9NVV4	0.550667
NCAPH	Q15003	0.548333
MRPS14	O60783	0.547333

MCM4	P33991	0.545333
HTT	P42858	0.543667
HACD2	Q6Y1H2	0.543667
BRIX1	Q8TDN6	0.539333
RBBP5	Q15291	0.537667
EIF1B	O60739	0.531
FANCI	Q9NVI1	0.527667
NEMF	O60524	0.527
DDX56	Q9NY93	0.525667
TACC1	O75410	0.524667
MKI67	P46013	0.523
GCLC	P48506	0.521
DNAJA1	P31689	0.519333
NOP53	Q9NZM5	0.515333
SPAST	Q9UBP0	0.512667
CDK4	P11802	0.512
LPGAT1	Q92604	0.510667
AURKB	Q96GD4	0.51
KIAA0391	O15091	0.504
FASTKD2	Q9NYY8	0.502
MRPL2	Q5T653	0.501667
MCCC2	Q9HCC0	0.498
CTR9	Q6PD62	0.497333
TUBG1	P23258	0.496333
GNL2	Q13823	0.494
HSPA2	P54652	0.493667
ZC3H13	Q5T200	0.493667
CHMP1B	Q7LBR1	0.493333
ATG4B	Q9Y4P1	0.493
AHSA1	O95433	0.492
DDX47	Q9H0S4	0.491333
MAD2L1	Q13257	0.491333
MCMBP	Q9BTE3	0.491
MCM2	P49736	0.490667
MCM6	Q14566	0.488333
NUCB1	Q02818	0.486333
FAM8A1	Q9UBU6	0.482667
NDUFS2	O75306	0.481
PCM1	Q15154	0.479333
MRPL47	Q9HD33	0.476667
HARS2	P49590	0.475667
HAT1	O14929	0.475
NDUFV1	P49821	0.471667
EIF2B4	Q9UI10	0.469
MRPL38	Q96DV4	0.468
JMJD6	Q6NYC1	0.466
HEATR5A	Q86XA9	0.458667
UBL5	Q9BZL1	0.458333
OXA1L	Q15070	0.456333
WRAP53	Q9BUR4	0.455333

KRT81	Q14533	0.454333
CDK2	P24941	0.452667
MRPS30	Q9NP92	0.439
MRPL22	Q9NWU5	0.438667
SPC24	Q8NBT2	0.434
PDCL3	Q9H2J4	0.433667
UQCC1	Q9NVA1	0.432667
GTF3C3	Q9Y5Q9	0.431
MAIP1	Q8WWC4	0.428
NMD3	Q96D46	0.425
SUCLA2	Q9P2R7	0.424667
GNL3L	Q9NVN8	0.424333
PYCARD	Q9ULZ3	0.422333
MCM5	P33992	0.422
SRXN1	Q9BYN0	0.421667
CRAT	P43155	0.419
GPRC5C	Q9NQ84	0.418667
MYO10	Q9HD67	0.418
PCNA	P12004	0.415
RIF1	Q5UIP0	0.413667
MRPS18B	Q9Y676	0.411667
CRNKL1	Q9BZJ0	0.410667
MASTL	Q96GX5	0.407333
CCDC97	Q96F63	0.397
DCAF13	Q9NV06	0.378667
KIF11	P52732	0.370333
GTF3C5	Q9Y5Q8	0.368
DHFR	P00374	0.363
NFU1	Q9UMS0	0.360667
CLPX	O76031	0.349667
MRPS21	P82921	0.348
KPNA2	P52292	0.347
CPS1	P31327	0.346667
SLC12A2	P55011	0.345
CYP4F11	Q9HBI6	0.334667
HMGCS1	Q01581	0.33
DNMT1	P26358	0.321
TK1	P04183	0.310667
NDUFS8	O00217	0.300333
CA8	P35219	0.296667
MICU2	Q8IYU8	0.295667
PLK1	P53350	0.293667
TBRG4	Q969Z0	0.283667
SHCBP1	Q8NEM2	0.249333
NSA2	O95478	0.238
GLDC	P23378	0.234
COQ8B	Q96D53	0.232
RRM2	P31350	0.211333
CES1	P23141	0.165667
SPAG5	Q96R06	0.127333